Available online at www.sciencedirect.com

ScienceDirect

MATTER AND RADIATION AT EXTREMES

Matter and Radiation at Extremes 1 (2016) 213–223

www.journals.elsevier.com/matter-and-radiation-at-extremes

Research Article

Investigation of spherical and concentric mechanism of compound droplets

Meifang Liu [a,**], Lin Su [a], Jie Li [a], Sufen Chen [a], Yiyang Liu [a], Jing Li [a], Bo Li [a], Yongping Chen [b,c], Zhanwen Zhang [a,*]

[a] *Research Center of Laser Fusion, China Academy of Engineering Physics, Mianyang, 621900, China*
[b] *School of Energy and Power Engineering, Yangzhou University, Yangzhou, Jiangsu, 225127, China*
[c] *Key Laboratory of Energy Thermal Conversion and Control of Ministry of Education, School of Energy and Environment, Southeast University, Nanjing, Jiangsu, 210096, China*

Received 22 January 2016; revised 31 May 2016; accepted 5 July 2016
Available online 16 July 2016

Abstract

Polymer shells with high sphericity and uniform wall thickness are always needed in the inertial confined fusion (ICF) experiments. Driven by the need to control the shape of water-in-oil (W1/O) compound droplets, the effects of the density matching level, the interfacial tension and the rotation speed of the continuing fluid field on the sphericity and wall thickness uniformity of the resulting polymer shells were investigated and the spherical and concentric mechanisms were also discussed. The centering of W1/O compound droplets, the location and movement of W1/O compound droplets in the external phase (W2) were significantly affected by the density matching level of the key stage and the rotation speed of the continuing fluid field. Therefore, by optimizing the density matching level and rotation speed, the batch yield of polystyrene (PS) shells with high sphericity and uniform wall thickness increased. Moreover, the sphericity also increased by raising the oil/water (O/W2) interfacial tension, which drove a droplet to be spherical. The experimental results show that the spherical driving force is from the interfacial tension affected by the two relative phases, while the concentric driving force, as a resultant force, is not only affected by the three phases, but also by the continuing fluid field. The understanding of spherical and concentric mechanism can provide some guidance for preparing polymer shells with high sphericity and uniform wall thickness.

PACS codes: 64.70.pv; 68.05.Gh

Keywords: Compound droplet stability; Compound droplet deformation; Sphericity; Wall thickness uniformity; Interfacial tension; Density matching

1. Introduction

In recent years, laser inertial confined fusion (LICF), one of the most promising methods to control the reaction of nuclear fusion, has attracted a great deal of interest due to its cleanness and efficiency [1]. In LICF experiments, several kinds of polymer shells such as polystyrene (PS), deuterated PS, poly(α-methylstyrene) (PAMS) and divinylbenzene (DVB) foam shells can be used for preparing LICF targets [2–4]. It has been reported that the shape and symmetry of these polymer shells, specifically, the sphericity and wall thickness uniformity are important to the symmetry and hydrodynamic stability in implosions, thus there are stringent specifications on the sphericity and wall thickness uniformity of these shells [5,6].

Generally, these shells are prepared by the microencapsulation technique, as shown in Fig. 1, in which compound droplets with a W1/O or O1/W structure are formed firstly, and

* Corresponding author.
** Corresponding author.
E-mail addresses: liumeifang@caep.cn (M. Liu), bjzzw1973@163.com (Z. Zhang).
Peer review under responsibility of Science and Technology Information Center, China Academy of Engineering Physics.

http://dx.doi.org/10.1016/j.mre.2016.07.002

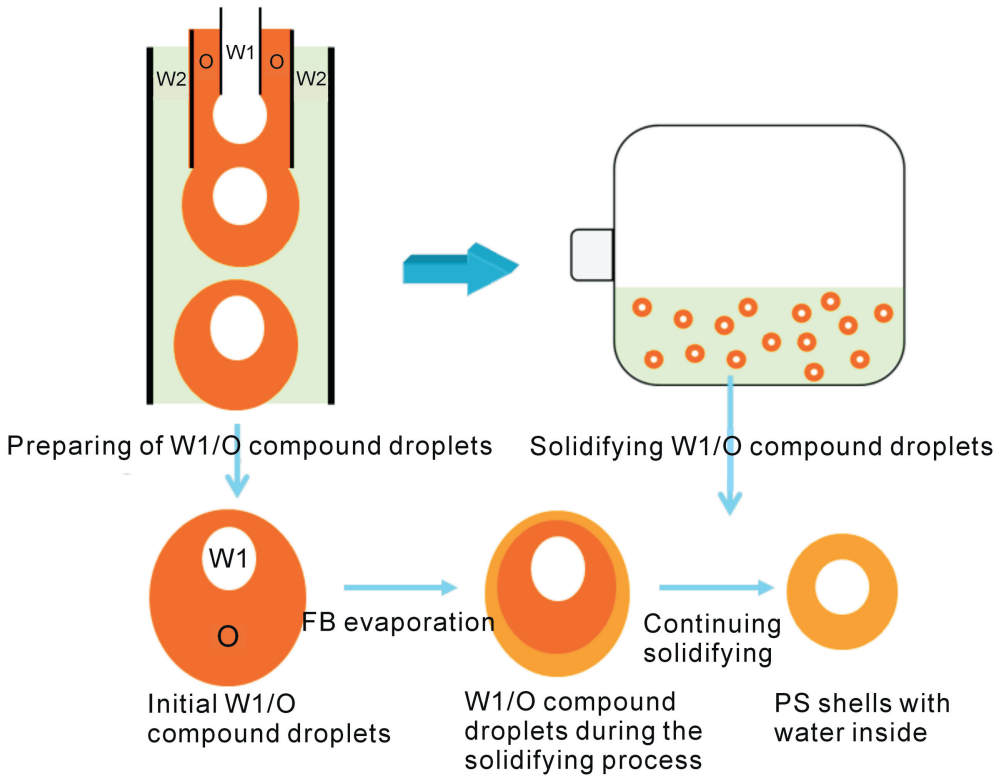

Fig. 1. Schematic of preparing PS shells.

then the solvent in the middle phase is removed by evaporation during solidifying process. Obviously, the key constraint in the sphericity and uniform wall thickness of the shells in turn requires a spherical and centered core compound droplet before its solidifying [7,8]. An initial compound droplet generated by a triple orifice droplet generator is not a perfect spherical drop and the inner phase is not in the center of the middle phase. Due to gravitational force, drag force and so on, the non-spherical and eccentric phenomenon probably becomes worse during the solidifying process. By increasing the wall thickness, both the deformation of the O phase and the moving space of the inner phase increase, thus it becomes more difficult to make a thick-walled compound droplet be spherical and concentric.

Over the past two decades, in order to obtain polymer shells with high sphericity and uniform wall thickness, a lot of research work has been done to control the deformation of droplets. It is found that there are many factors, such as the interfacial tension, density and viscosity, influencing the deformation of droplets [9–12]. For a droplet without inner phase, a simple theory of Taylor shows that the deformation (δ) is [13]:

$$\delta = \frac{D_{\max} - D_{\min}}{D_{\max} + D_{\min}} = \frac{19\lambda + 16}{16\lambda + 16} C_a. \tag{1}$$

where λ is the ratio of the droplet viscosity to the continuous phase viscosity, C_a is the so-called capillary number, defined as

$$C_a = \frac{\eta_c \nu r}{\gamma} \tag{2}$$

where η_c is the viscosity of the continuous fluid phase, ν is the applied shear-rate, r is the undeformed droplet radius, and γ is the interfacial tension of the interface.

Moreover, Cook et al. estimated that the maximum out-of-roundness (δ_{MOOR}) of a drop without inner phase in a continuous phase is related to physical properties such as the density matching level, interfacial tension and viscosity, *i.e.* [9],

$$\delta_{MOOR} = \frac{5gr^3\Delta\rho}{4\gamma}, \tag{3}$$

where g is the acceleration of gravity (9.8 $m \cdot s^{-2}$) and $\Delta\rho$ is the density difference between the droplet and the continuous fluid phase.

$$\delta_{MOOR} \cong \frac{8\eta_c \nu r^2}{\gamma}. \tag{4}$$

For W1/O compound droplet, there are three phases and two interfaces, the structure of which is more complicated than that of a droplet without inner phase. Moreover, the W1 phase can move randomly in the O phase in the initial range of the solidifying process. Therefore, it is difficult to control the shape of compound droplets. It is reported that the physical properties of the W1, O and W2 phases such as their density and viscosity, and the properties of the interfacial film such as the interfacial tension, interfacial film strength and interfacial

rheology, probably have significant influences on the deformation of compound droplets [12]. Moreover, the continuing fluid field also has an important effect on their deformation [14]. However, neither the relationships between these parameters and the sphericity or the wall uniformity nor the possible mechanisms are clearly established. Fundamental research in investigation of the role of these principal parameters in the resulting sphericity and wall thickness uniformity will lead to optimized microencapsulation technique and improved yield of polymer shells which meet stringent specifications. Therefore, in this paper, the effects of the density matching, interfacial tension, and continuing fluid field on the deformation of compound droplets are investigated and the relative mechanisms are also discussed.

2. Experiment

2.1. Materials

The following materials used in the experiment were all used: PS (M_w = 250 kg•mol^{-1}, ρ_s = 1.05 g•cm^{-3}, Acros Organics Inc.), poly(vinyl alcohol) (PVA) (M_w = 13–23 kg•mol^{-1}, 87%–89% mole hydrolyzed, Aldrich Company), poly(acrylic acid) (L-PAA, M_w = 450 kg•mol^{-1}, H-PAA, M_w = 1000 kg•mol^{-1}, Polymer Source) and anhydrous calcium chloride ($CaCl_2$) (Chengdu Kelong Chemical Reagent Factory) were all used as originally received without further purification. Fluorobenzene (FB, Shanghai Jingchun Reagent Ltd.) was purified by distillation. Distilled, deionized water was used in the preparation of all aqueous phases.

2.2. Preparation of PS shells

PS shells were prepared by the microencapsulation technique. Details of the fabrication process were in Ref. [15]. As shown in Fig. 1, the W1, O and W2 phases were delivered into the microfluidic flow focusing device by three syringes, which were controlled by three pumps, respectively. The W1 phase left the W1 tube and was broken-up and surrounded by the O phase. Then, the encapsulated drop of the W1 phase surrounded by the O phase was stripped off from the W2 phase, forming the W1/O compound droplets in the W2 phase. To obtain PS shells, the W1/O compound droplets were collected in an 800 ml cylindrical flask filled with 150 ml of the W2 solution. Then, the flask was sent to a heated water bath and gently rotated horizontally for about 2 days to make FB evaporate. After the removal of FB, the PS shells containing the interior water drop were transferred to another beaker and then washed several times with deionized water and ethanol to remove residuals on the outer surface. Finally, these thoroughly washed PS shells were dried at 45 °C at atmospheric pressure for at least 3 days.

To reduce possible effects of droplets size on the deformation, the inner diameter (ID) and outer diameter (OD) of the W1/O compound droplets in a batch were controlled by adjusting the W1, O, and W2 flow rates. The experimental results show that the variations of ID and OD in a batch were both in the range of 30 μm.

2.3. Characterization of experiment samples

2.3.1. Density

The densities of the W1, O and W2 phases were measured precisely by a densitometer (Anton Paar®, DMA 5000, 10^{-6} g•cm^{-3} accuracy) from 5 °C to 70 °C at intervals of 5 °C.

Due to high viscosity and low fluidity of PS/FB solution with high mass fractions of more than 30%, it was difficult to measure its density by the densitometer. Therefore, to obtain the density of PS/FB solution with high mass fractions, an exponential fit was used to correlate the mass fraction of the PS/FB solution with its density. The coefficient of determination with the density of the solution at 55 °C was more than 0.999, while its P-value was less than 0.001, which indicated that the fit correlated well. The average density of the W1/O compound droplets ($\rho_{w1/o}$) during the solidifying process can be calculated [16,17].

2.3.2. Viscosity

The viscosities of the W1, O and W2 phases were measured precisely by a microviscometer (Anton Paar®, Lovis 2000M, 10^{-3} mPa s accuracy) from 5 °C to 70 °C at intervals of 5 °C.

2.3.3. Interfacial tension

The interfacial tensions of these different solutions were measured by an interfacial tensiometer (Kruss, DSA25) via the pendant drop method. The diameter of the needle used for the measurement was 0.48 mm.

2.3.4. Hydrodynamic radius (R_h)

Dynamic light scattering (DLS) measurements were made with Zetasizer Nano ZS at 25 °C.

2.3.5. Morphology and dimension of W1/O droplets

The morphology of W1/O compound droplets was characterized by a digital microscope. The OD and ID of W1/O compound droplets in the W2 phase were obtained from these micrographies. The initial thickness of the O layer (t_{ol}) in the W1/O compound droplets could be calculated by the OD and ID values. Therefore, the dimension of the resulting PS shells can be estimated. The OD and wall thickness (t_w) of the PS shells were characterized by a measuring microscope [18]. For each batch, at least 40 PS shells were randomly picked up from about 120 PS shells for this characterization.

2.3.6. Sphericity and wall thickness uniformity of PS shells

For shells with the same diameter and same wall thickness, the out-of-roundness (δ_{OOR}) is defined as the difference between the maximum and minimum outer radius of a torus projected from the PS shells in six directions, which is used to characterize the sphericity of PS shells. The maximum variation of wall thickness (Δt_w) in the six directions, defined as the deduction of the minimum wall thickness from the maximum

one, is used to characterize the wall thickness uniformity of the PS shells [15,19].

Here, δ_{OOR} and Δt_w are calculated by

$$\delta_{OOR} = (D_{max} - D_{min})/2 \quad (5)$$

$$\Delta t_w = t_{w(max)} - t_{w(min)} \quad (6)$$

where D_{max} and D_{min} are the maximum and minimum outer diameters of a particular PS shell, respectively; $t_{w(max)}$ is the maximum value of the twelve measured wall thicknesses of a particular PS shell, while $t_{w(min)}$ is the minimum value.

3. Results and discussions

3.1. Density matching of the key stage

Since 1990s, density matching has been a research focus in the production of polymer shells with uniform wall thickness and good sphericity. However, the densities of the O phase and the W1/O compound droplets always change because of the removal of organic solvent in the O phase. It is difficult to keep the density matching constant. Therefore, the relationship between the density matching and the resulting wall uniformity or the sphericity and the possible mechanism underlying were not well understood in the past.

As shown in Fig. 2, the viscosity of the O phase increases exponentially with increasing PS mass fraction, while the fluidity of the O phase decreases. With the solidifying process continuing, the FB dissolves in the water and evaporates, therefore the mass fraction of PS in the O phase increases and its deformation ability decreases. Therefore, when the mass fraction of PS in the O phase reaches the extent of ~50%, the effects of gravity and buoyancy on the deformation of droplets become negligible. Obviously, the density matching should be controlled in the range of low PS concentrations (<40%), which is regarded as the key stage of controlling the density matching.

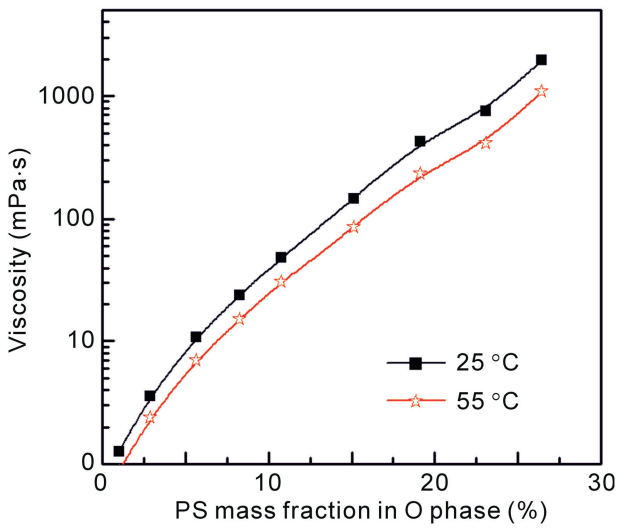

Fig. 2. Effects of PS mass fraction on the viscosity of PS/FB solution.

Our study has confirmed that the quality of PS shells is significantly affected by the density matching between the W1/O compound droplets and the W2 phase [15]. As shown in Fig. 3, with the density of the W1/O compound droplets being almost equal to or a little lower than that of the W2 phase, the gravity can be balanced by the buoyancy, therefore the W1/O compound droplets can follow with the flow of the W2 phase in the flask. Good dispersion and sufficient tumbling of the W1/O compound droplets could occur during the solidifying process, resulting in uniform wall thickness [14,20,21]. With the density of W1/O compound droplets being lower than that of the W2 phase, it is observed that the W1/O droplets cannot drop down, but float near the surface of the W2 phase, agglomerate together and always stay in one place during the solidifying process. The poor dispersion of the W1/O compound droplets in the W2 phase and their insufficiently tumbling during the solidifying process make the droplets collide easily, resulting in some PS pellets and some twin or triplet PS shells. With the density of W1/O compound droplets being much higher than that of the W2 phase, the W1/O compound droplets sink down to the down side of the flask, float up by the rotation of the flask, but then drop down quickly due to gravity. The insufficient tumbling leads to a lower centering force within each droplet, resulting in poor uniformity of the wall thickness.

The effect of the density matching between W1 and O phases on the quality of PS shells is similar to that between W1/O compound droplets and W2 phase. As shown in Fig. 4, without good density matching between the W1 and O phases, the internal water drop tends to eccentrate from the oil layer shell, probably due to the role of gravity and buoyancy [21]. The centering force from the droplet tumbling may not be so strong as to suppress the sinking or floating tendencies of the internal water drop, resulting in a poor wall thickness uniformity of the resulting PS shells. However, the density matching levels between the W1 and O phases in a relatively broad range (−0.019–0.017 g·cm^{-3}) have a small effect on the sphericity.

From the experimental results, it is clear that, the batch yield of PS shells with a uniform wall thickness increases by improving the density matching levels among the three phases into the optimum ranges, due to better symmetry of W1/O compound droplets and more adequate tumbling of W1/O compound droplets in W2 phase during the solidifying process. Compared with the wall thickness uniformity, the sphericity of PS shells is a little less sensitive to the density matching.

3.2. Balance between interfacial tension and compound droplets formation as well as stability

For a W1/O compound droplet with the outer and inner radius R and r, respectively, suspended in a W2 phase, the interfacial tension between W1 and O is $\gamma_{(W1/O)}$ and that between fluids O and W2 is $\gamma_{(O/W2)}$. When the gravitational forces do not strongly influence the interface shape, the

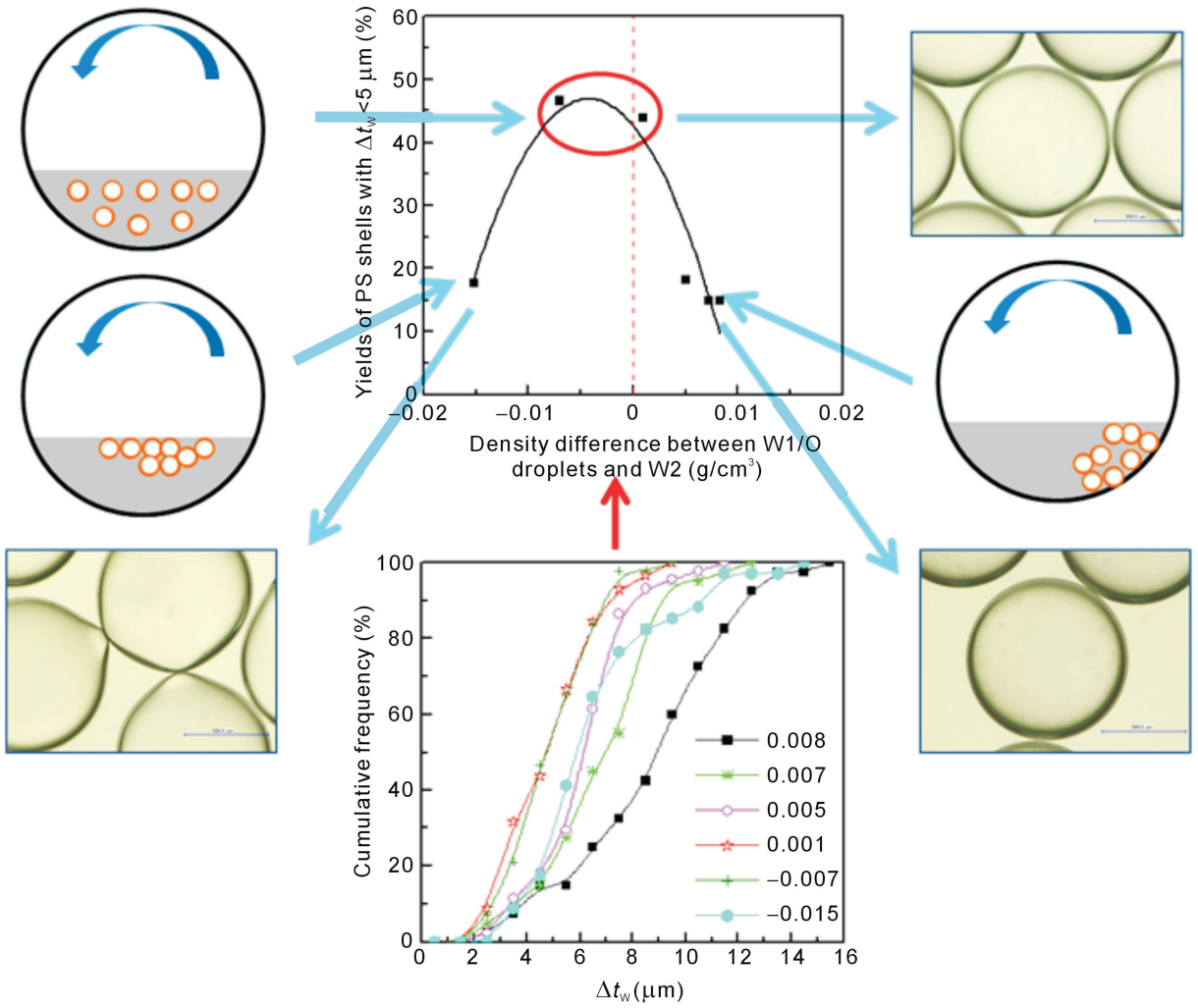

Fig. 3. Effects of the density matching level between W1/O droplets and W2 phase on the quality of PS shells.

Young–Laplace equation describes the normal stress balance as [22].

$$P_O = P_{W2} + \frac{2\gamma_{(O/W2)}}{R} \tag{7}$$

$$P_{W1} = P_{W2} + \frac{2\gamma_{(O/W2)}}{R} + \frac{2\gamma_{(W1/O)}}{r} \tag{8}$$

where P_{w2} is the absolute pressure in the W2 phase, P_o is the absolute pressure in the O phase and P_{w1} is the absolute pressure in the W1 phase. Obviously, the larger the interfacial tension is, the stronger the force pushing inward into the droplet will be [23]. The increase of the interfacial tension would make the initial compound droplet be more spherical. However, the change in the Gibbs free energy (ΔG) during the generation is

$$\Delta G = \Delta A\gamma - T\Delta S \tag{9}$$

where ΔA is the increase in interfacial area when the bulk oil produces a large number of droplets, T is the temperature and ΔS is the entropy. The increase of the interfacial tension brings about an increase in the Gibbs free energy for the surface area change, which indicates that more energy is required to produce the droplets. Therefore, though it is promising to increase the interfacial tension to improve the sphericity, the increase probably also brings some negative effects on the formation of the droplets.

To improve the sphericity, PVA is replaced by different PAAs in the W2 phase. The experimental results show that the interfacial tension at 25 °C increases no matter whether the molecular weight of PAA is low or high (see Table 1). However, when L-PAA is used in the W2 phase, it is difficult to detach W1/O compound droplets from the middle tube. The diameter and wall thickness of W1/O compound droplets are also hard to control. The distribution of diameter and wall thickness of these compound droplets become broad, as shown in Fig. 7. Moreover, two or more compound droplets coalesce to form bigger droplets in a short time after the generation, indicating that their stability is poor. A stable W1/O compound droplet is a critical first step in the preparation of polymer shells. Obviously, it is necessary to reduce negative effects

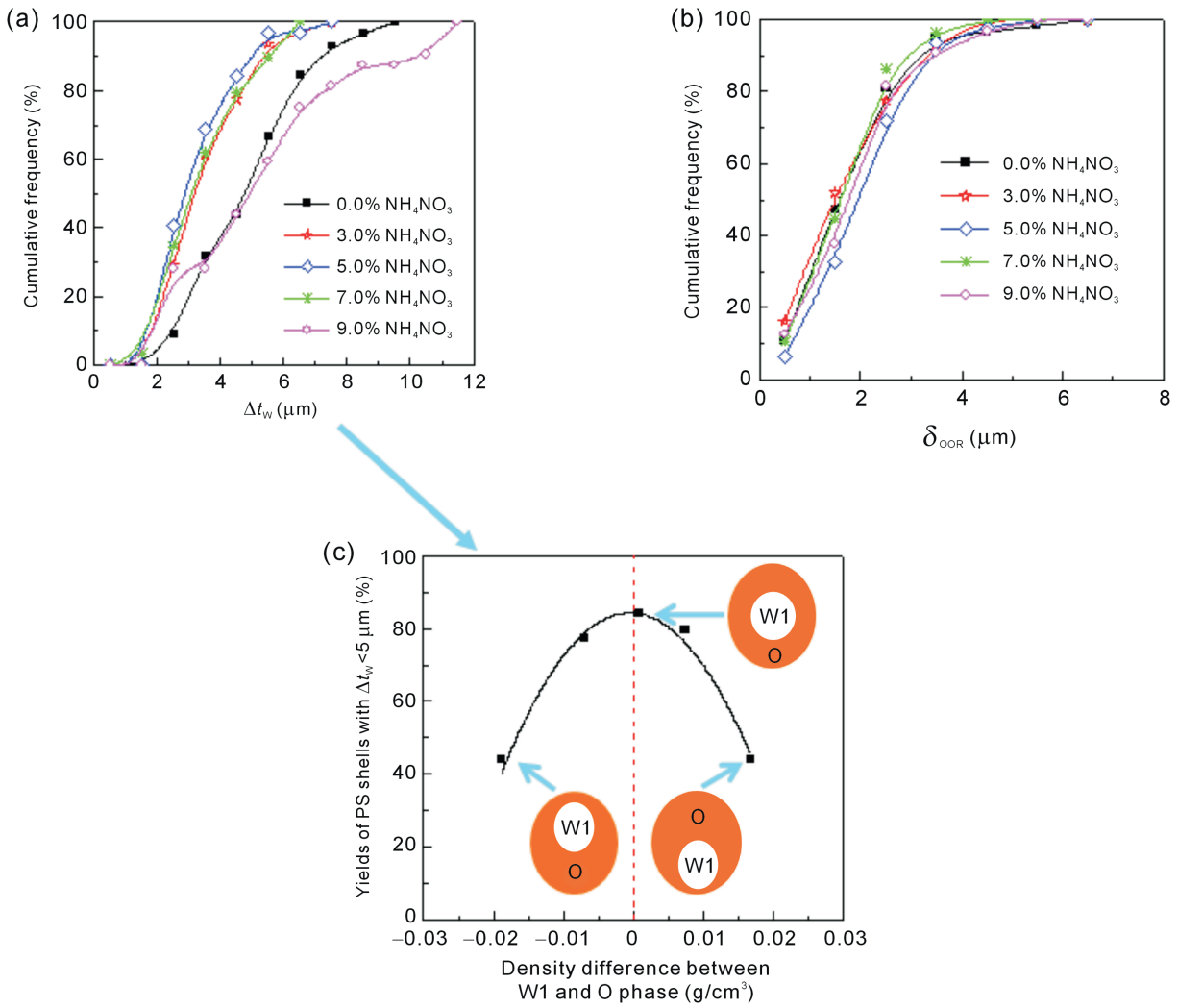

Fig. 4. Effects of the density matching level between the W1 and O phases on the quality of PS shells: (a) wall thickness uniformity, (b) sphericity and (c) relationships between the density matching level between W1 and O phases and the yields of PS shells with $\Delta t_w < 5$ μm.

Table 1
Interfacial tensions of O/W2 interphases at room temperature (25 °C).

Solution	Interfacial tension (mN/m)
Water/FB	21
PVA/FB	2
L-PAA/FB	19
H-PAA/FB	22

from the increase of the interfacial tension on the droplets formation and the droplets stability.

As shown in Fig. 5, the formation of a single droplet is mainly dominated by the gravity force (F_G), buoyancy force (F_B), viscous shear force (F_V), momentum force (F_M), static pressure difference force (F_S), and interfacial force (F_γ) [24–27]. From Fig. 1, the W1 single droplet is formed by breaking up the W1 phase and then W1/O compound droplet is formed by breaking up the O phase when the W1 droplet moves to the tip of the O tube. Since PAA is in the W2 phase, the formation of W1 single droplet should be unaffected. As

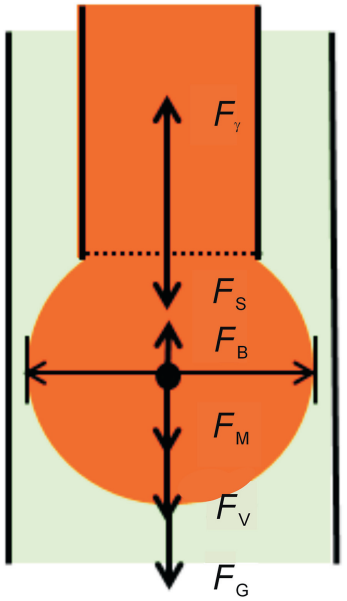

Fig. 5. Schematic of forces acting on a droplet.

shown in Fig. 6, the density of the W2 phase with L-PAA is a little less than that of the W2 phase with PVA at the generation temperature of the W1/O droplets (25 °C), while their viscosities are almost the same. So the increase of the interfacial tension, which cannot be balanced by the viscous shear force since the viscosity of L-PAA solution is close to that of the PVA solution and the adjustable range of flow rates is limited.

On the contrary, for the H-PAA solution, the W1/O compound droplets prepared by H-PAA solution is monodisperse and the stability is good (see Fig. 7), probably due to the increase of the viscosity and longer chain length. As shown in Fig. 6, the viscosity of H-PAA solution is about 12 times as high as that of the PVA solution at the generation temperature of the W1/O droplets (25 °C), where increasing the viscous shear force can balance the increase of the interfacial tension. Moreover, the hydrodynamic radius (R_h) of the H-PAA solution is 1813 nm while that of the L-PAA solution is 881 nm, so the chain length is long enough that a steric stabilization may play a more significant role on the stability of the W1/O compound droplets.

The effect of H-PAA on the quality of PS shells is shown in Fig. 8. Whether the diameter is 900 μm or 1900 μm, the sphericity of PS shells prepared by H-PAA solution is better, probably due to the increase of interfacial tension. For the wall thickness, there is no significant effect of H-PAA on PS shells with 900 μm diameter, but PS shells with 1900 μm diameter prepared by the H-PAA solution shows better wall thickness uniformity. Obviously, the different effects of H-PAA on the wall thickness uniformity of the PS shells cannot result from the agitation and the solidifying temperature since they are the same. These PS shells are prepared in the same process, and the only difference is the replacement of PVA by H-PAA in the W2 phase, which alters the properties of the W2 phase and O/W2 interfaces during the solidifying process.

As shown in Fig. 9, whether the diameter is 900 μm or 1900 μm, the decrease in the density matching level between the W1/O compound droplets and W2 phases is ~0.1 g cm^{-3} when the PVA is replaced by H-PAA, unfavorable to the wall thickness uniformity. On the other hand, 8.20% PS was used as the O phase for preparing 900 μm shells while 10.50% PS for 1900 μm shells. The viscosity of 8.20% PS is 15.0 mPa s, which is close to that of the PAA solution while that of 10.50% PS is higher (see Table 2). Therefore, the viscosity ratios of the O to W2 phases are 1.2 and 2.4, respectively. It has been reported that the appropriate viscous shear force can make compound droplet become centering, but it can also make them eccentric when the viscous shear force is large [28,29]. Moreover, Takagi et al. pointed out that the concentricity of poly(α-methylstyrene) (PAMS) shells was improved by increasing the interfacial tension while McQuillan et al. advised that a decrease in the interfacial tension might make the oscillation magnitude larger, thus hastening the centering [3,30]. Therefore, different effects of H-PAA on wall thickness uniformity of PS shells with 900 μm and 1900 μm diameters are probably due to the decrease of the density matching level, the increase of the interfacial tension and different viscosities of the O phases. The mechanism will be investigated further.

3.3. Effects of viscous shear force on concentricity and deformation

As mentioned above, the viscous shear force plays a paradoxical role on concentricity. During the solidifying process, the flask rotates around the horizontal axis and the rotation speed is one of the most important factors affecting the viscous shear force [14,31]. The velocity distribution fields in the gas and liquid on the vertical cross section of the flask at different rotation speed were calculated by the software ANSYS FLUENT. Fig. 10 displays the velocity distribution fields and the collision number of the droplets in the continuing fluid field at 20 rpm. As shown in Fig. 10(a), there are two vortices (vortex A and vortex B) in the liquid field. These vortices play

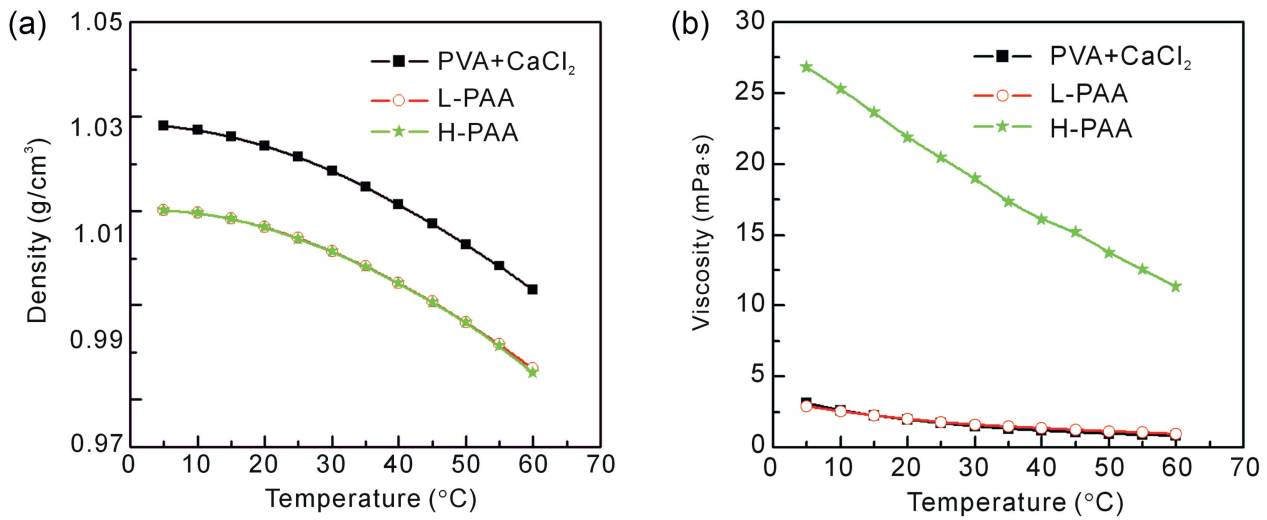

Fig. 6. (a) Density and (b) viscosity profiles of different W2 phases at different temperature.

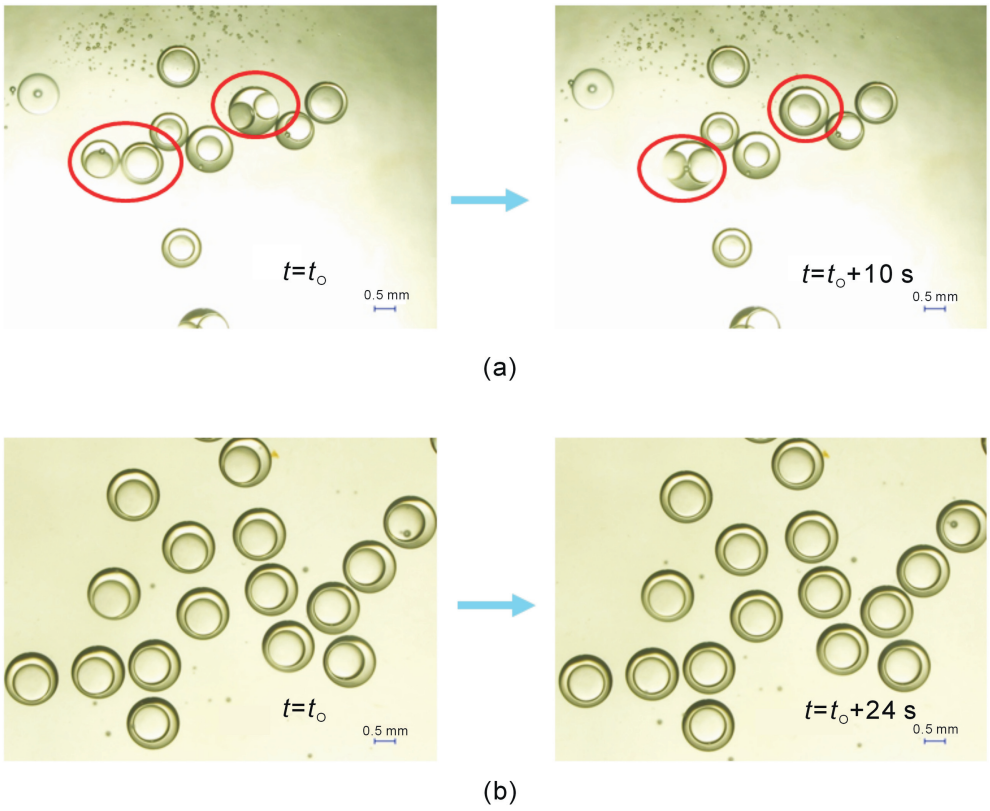

Fig. 7. Stability of W1/O compound droplets prepared by (a) L-PAA and (b) H-PAA.

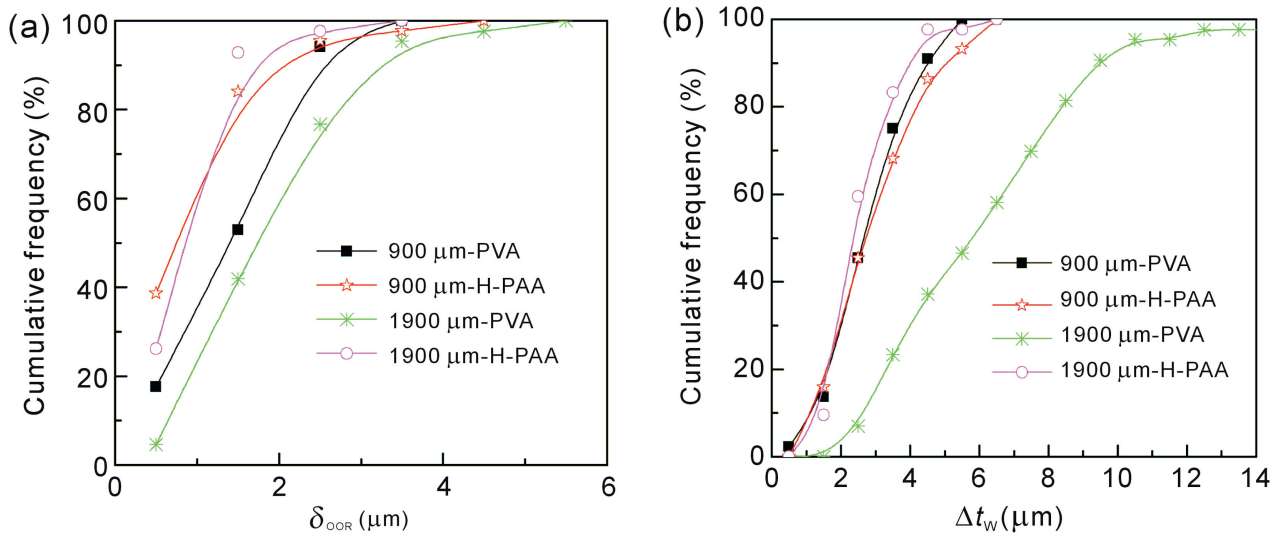

Fig. 8. Effects of the interfacial tension between O and W2 phases on the quality of PS shells: (a) sphericity and (b) wall thickness uniformity.

an important role on the dispersion of the W1/O compound droplets in W2 phase. With increasing the rotation speed, there will be more vortices, improving the dispersion. However, the existence of more vortices also increases the degree of mess of the W2 phase, thus increases the collision probability of the droplets.

According to the calculated results, the lowest collision number appears at 40 rpm, which benefits preparing shells with good sphericity and wall thickness uniformity. As shown in Fig. 11, the experimental results show that the sphericity and wall thickness uniformity of PS shells prepared at 25 rpm and 45 rpm are almost the same in the H-PAA system and

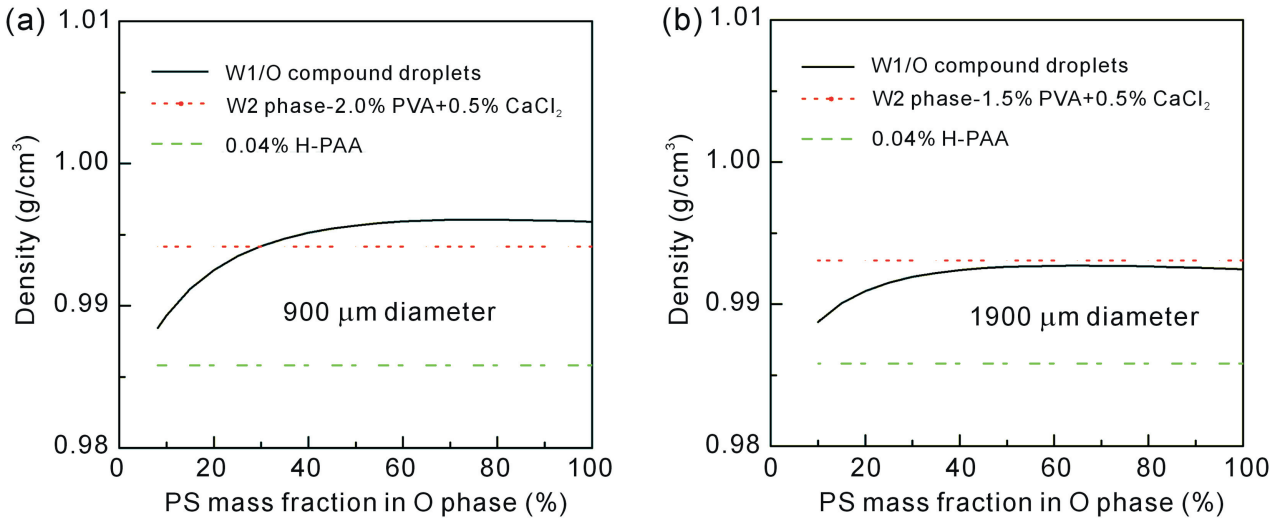

Fig. 9. Density profiles of different W2 phases and W1/O compound droplets with (a) 900 μm and (b) 1900 μm diameter during the solidifying process at 55 °C.

Table 2
Viscosities of O and W2 phases at the generation temperature (25 °C) and solidifying temperature (55 °C).

Sample	Viscosity at 25 °C (mPa•s)	Viscosity at 55 °C (mPa•s)
8.20% PS	23.8	15.0
10.50% PS	48.5	30.0
2.00% PVA	1.7	0.9
0.04% L-PAA	1.8	1.0
0.04% H-PAA	20.4	12.6

much better than those at 5 rpm and 65 rpm, which is probably due to lower collision number and appropriate viscous shear force. At 5 rpm, the viscous shear force is so small that it has little effect on the movement of the droplets. These droplets agglomerate together and always stay in one place, which is unfavorable to reduce the negative of gravity, resulting in poor sphericity and nonuniform wall thickness. By increasing the rotation speed, the viscous shear force also increases. When increases to a certain extent, it will make the droplets deform seriously, resulting in poor sphericity and wall thickness uniformity.

4. Conclusions

PS shells were prepared by microencapsulation technique and the effects of the density matching level, the interfacial tension and the rotation speed on their sphericity and wall thickness uniformity are discussed and some insights are obtained: (i) The centering of W1/O compound droplets, the location and movement of W1/O compound droplets in W2 phase are significantly affected by density matching between W1 and O phases, and that between W1/O compound droplets and W2 phase, respectively. The batch yield of PS shells with a uniform wall thickness increases by improving the density matching levels into the optimum ranges, due to better symmetry of W1/O compound droplets and more adequate

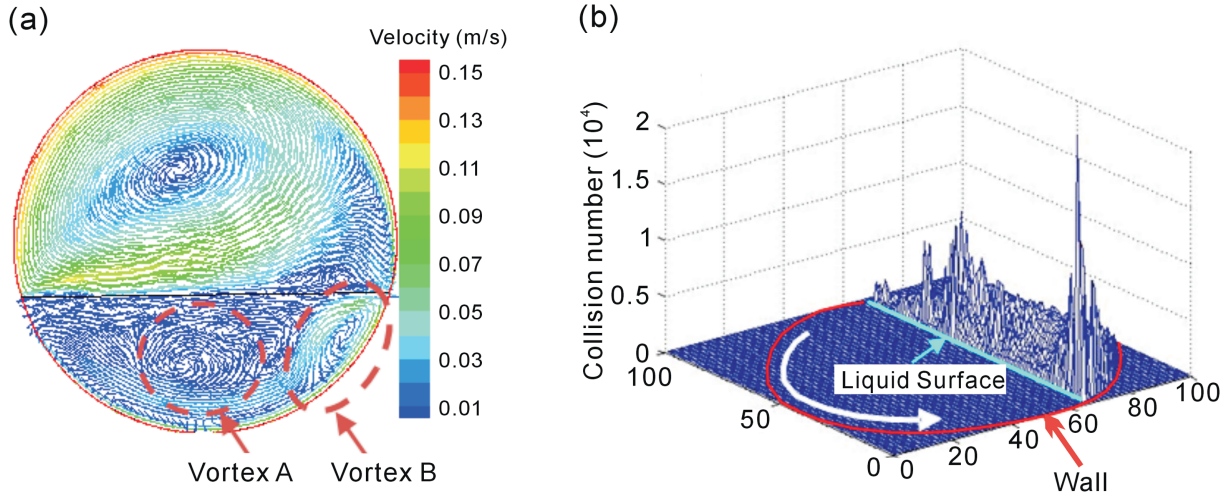

Fig. 10. (a) Velocity distributions and (b) collision number of the droplets on the vertical cross section of the horizontal rotating cylindrical flask at 20 rpm.

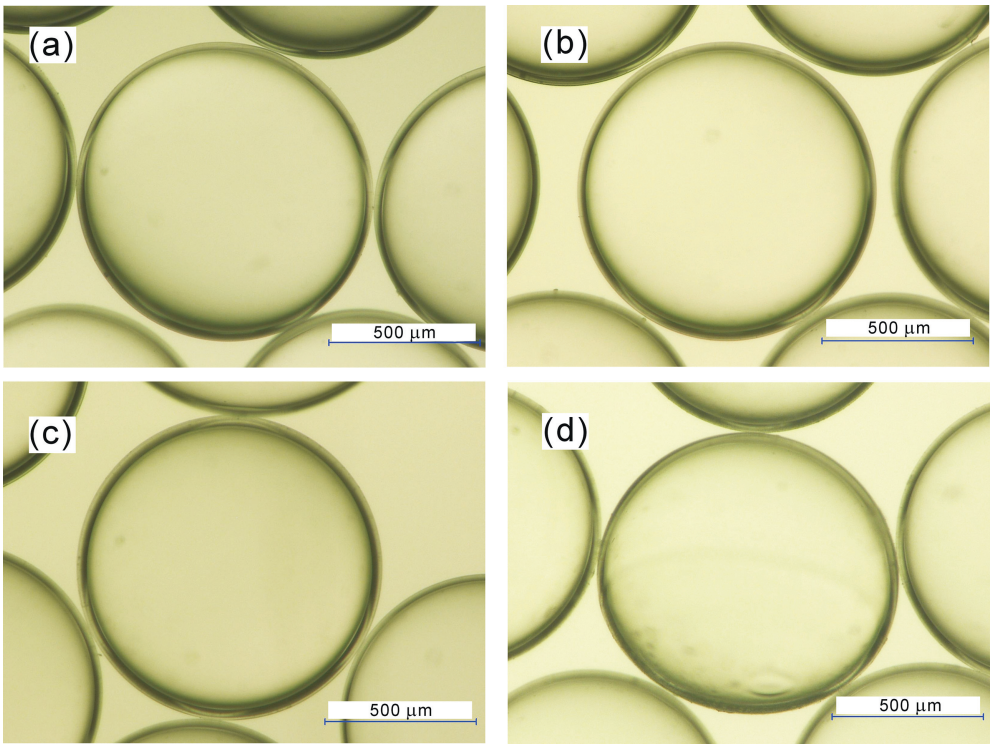

Fig. 11. Microphotograph of the obtained PS shells prepared at different rotation speed: (a) 5 rpm, (b) 25 rpm, (c) 45 rpm and (d) 65 rpm.

tumbling of W1/O compound droplets in W2 phase. Compared with the wall thickness uniformity, the sphericity is a little less sensitive to density matching. (ii) Since the interfacial tension is the driving force of making a droplet be spherical, increasing the interfacial tension between O and W2 phases ($\gamma_{(O/W2)}$) improves the sphericity. However, it also increases the upward force during the formation of the droplets, which requires larger viscous shear force to detach the droplets. Moreover, negative effects of the interfacial tension increase on the droplet stability should be avoided. (iii) The viscous shear force plays a paradoxical role on the concentricity. Adjusting the rotation speed to an optimum range can improve the sphericity and wall thickness uniformity, due to lower collision number and appropriate viscous shear force. Further research is still needed to establish, at a fundamental level, the effects of the interfacial tension on the wall uniformity, the effects of the properties of interfacial film such as the interfacial film strength and interfacial rheology on the deformation, the balance between the centering and deformation, and so on.

Acknowledgments

The authors are grateful to the China Academy of Engineering Physics for financial support (2014B0302052) and National Natural Science Foundation of China (U1530260).

References

[1] A.M. Dunne, HiPER: Technical Background and Conceptual Design Report 2007, Science and Technology Facilities Council, Rutherford Appleton Laboratory, Central Laser Facility, 2007.

[2] K. Nagai, H. Yang, T. Norimatsu, H. Azechi, F. Belkada, et al., Fabrication of aerogel capsule, bromine-doped capsule, and modified gold cone in modified target for the Fast Ignition Realization Experiment (FIREX) project, Nucl. Fusion 49 (2009) 095028.

[3] P.R. Paguio, S.P. Paguio, C.A. Frederick, A. Nikroo, O. Acenas, Improving the yield of target quality Omega size PAMS mandrels by modifying emulsion components, Fusion Sci. Technol. 49 (2006) 743–749.

[4] C. Lattaud, L. Guillot, C.-H. Brachais, E. Fleury, O. Legaie, et al., Influence of a density mismatch on TMPTMA shells nonconcentricity, J. Appl. Polym. Sci. 124 (2012) 4882–4888.

[5] A.K. Tucker-Schwartz, Z. Bei, R.L. Garrell, T.B. Jones, Polymerization of electric field-centered double emulsion droplets to create polyacrylate shells, Langmuir 26 (2010) 18606–18611.

[6] N. Antipa, S. Baxamusa, E. Buice, A. Conder, M. Emerich, et al., Automated ICF capsule characterization using confocal surface profilometry, Fusion Sci. Technol. 63 (2013) 151–159.

[7] G. Randall, B. Blue, Preventing droplet deformation during dielectrophoretic centering of a compound emulsion droplet, Bull. Am. Phys. Soc. 57 (2012).

[8] G. Randall, B. Blue, Continuous dielectrophoretic centering of compound droplets, in: APS Meeting Abstracts, 2012, 41014.

[9] R.C. Cook, P.M. Gresho, K.E. Hamilton, Examination of some droplet deformation forces related to NIF capsules sphericity, J. Mosc. Phys. Soc. 8 (1998) 221–226.

[10] S. Kumar, V. Ganvir, C. Satyanand, R. Kumar, K. Gandhi, Alternative mechanisms of drop breakup in stirred vessels, Chem. Eng. Sci. 53 (1998) 3269–3280.

[11] H. Ren, S. Xu, S.T. Wu, Effects of gravity on the shape of liquid droplets, Opt. Commun. 283 (2010) 3255–3258.

[12] X. Qu, Y. Wang, Dynamics of concentric and eccentric compound droplets suspended in extensional flows, Phys. Fluids 24 (2012) 123302–123321.

[13] D. Megias-Alguacil, Interfacial tension determination of liquid systems in which one of the phases is non-Newtonian using a rheo-optical method, Meas. Sci. Technol. 22 (2011) 037002.

[14] B.W. Mcquillan, A. Greenwood, Microencapsulation process factors which influence the sphericity of 1 mm o.d. poly(a-methystyrene) shells for ICF, Fusion Technol. 35 (1999) 194–197.

[15] M.F. Liu, S.F. Chen, X.B. Qi, B. Li, R.T. Shi, et al., Improvement of wall thickness uniformity of thick-walled polystyrene shells by density matching, Chem. Eng. J. 241 (2014) 466−476.
[16] B. Cook, M. Takagi, S. Buckley, E. Fearon, A. Hassel, Organic solvent choice, in: Mandrel Development Update − l/98 to 12/98, 1999.
[17] S.F. Chen, L. Su, Y.Y. Liu, B. Li, X.B. Qi, et al., Density match during fabrication process of poly(α-methylstyrene) mandrels by microencapsulation, High Power Laser Part. Beams 24 (2012) 1561−1565.
[18] H. Huang, R.B. Stephens, D.W. Hill, C. Lyon, A. Nikroo, et al., Automated batch characterization of ICF shells with vision-enabled optical microscope system, Fusion Sci. Technol. 45 (2004) 214−217.
[19] M.F. Liu, S.F. Chen, Y.Y. Liu, L. Su, R.T. Shi, et al., Characterization of sphericity and wall thickness uniformity of thick-walled hollow microspheres, High Power Laser Part. Beams 26 (2014) 153−157.
[20] T. Norimastu, Y. Izawa, K. Mima, P.M. Gresho, Modeling of the centering force in a compound emulsion to make uniform plastic shells for laser fusion targets, Fusion Technol. 35 (1999) 147−156.
[21] M. Takagi, R. Cook, R. Stephens, J. Gibson, S. Paguio, Stiffening of PaMS mandrels during curing, Fusion Technol. 38 (2000) 50−53.
[22] N.J. Alvarez, L.M. Walker, S.L. Anna, A microtensiometer to probe the effect of radius of curvature on surfactant transport to a spherical interface, Langmuir 26 (2010) 13310−13319.
[23] J. Jiao, D.J. Burgess, Multiple emulsion stability: pressure balance and interfacial film strength, in: Multiple Emulsions, John Wiley & Sons, Inc., 2008, pp. 1−27.
[24] P.B. Umbanhowar, V. Prasad, D.A. Weitz, Monodisperse emulsion generation via drop break off in a coflowing stream, Langmuir 16 (2000) 347−351.
[25] J.H. Xu, G.S. Luo, G.G. Chen, J.D. Wang, Experimental and theoretical approaches on droplet formation from a micrometer screen hole, J. Membr. Sci. 266 (2005) 121−131.
[26] J.H. Xu, S.W. Li, W.J. Lan, G.S. Luo, Microfluidic approach for rapid interfacial tension measurement, Langmuir 24 (2008) 11287−11292.
[27] G. De Luca, F.P. Di Maio, A. Di Renzo, E. Drioli, Droplet detachment in cross-flow membrane emulsification: comparison among torque- and force-based models, Chem. Eng. Process. Process Intensif. 47 (2008) 1150−1158.
[28] T.G. Wang, A. Anilkumar, C. Lee, K. Lin, Core-centering of compound drops in capillary oscillations: observations on USML-1 experiments in space, J. Colloid Interface Sci. 165 (1994) 19−30.
[29] A. Anilkumar, A. Hmelo, T. Wang, Core centering of immiscible compound drops in capillary oscillations: experimental observations, J. Colloid Interface Sci. 242 (2001) 465−469.
[30] B.W. McQuillan, R. Paguio, P. Subramanian, M. Takagi, A. Zebib, Hydrodynamic issues in PAMS mandrel target fabrication, in: Third International Conference on Inertial Fusion Sciences and Applications, Monterey, CA, 2003.
[31] J. Streit, D. Schroen, Developmet of divinylbenzene foam shells for use as inertial fusion energy reactor targets, Fusion Sci. Technol. 43 (2003) 321−326.